Electromagnetic responses from planar arrays of dielectric nano-disks at overlapping dipolar resonances

N. Gandji, G. Semouchkin, and E. Semouchkina
Department of Electrical and Computer Engineering
Michigan Technological University,
Houghton, MI, USA
esemouc@mtu.edu

***Abstract*—Periodic arrays of dielectric nano-disk resonators are investigated to clarify the nature of their electromagnetic responses, in particular, the relation of light transmission to Kerker's conditions at overlapping dipolar resonances. It is concluded that periodicity and inter-resonator coupling define the observed responses.**

Keywords - directional scattering, dipolar resonances, dispersion diagrams, transmission bands

I. Introduction

Recently revealed opportunity to obtain directional scattering of light from dielectric nanoparticles due to interplay between two dipolar resonances, magnetic (MR) and electric (ER) ones, attracts a lot of attention. It was noticed [1], however, that directional forward scattering (FS) from dielectric spheres observed at overlapping of "tails" of MR and ER (1st Kerker's condition) was not strong enough for practical applications. In order to enhance scattering by shifting MR and ER closer in the frequency spectra, particles with other than spherical shape were investigated, in particular, spheroids [1] and flat disks with the aspect ratio of about 1:2 [2], in which frequencies of two resonances could coincide. In the case of coincidence, the 1st Kerker's condition could be fulfilled at the common resonance frequency that should lead to powerful FS at zero backward scattering (BS).

However, the data obtained at the studies of Kerker's related effects in arrays of silicon nano-disks [2, 3], cause some questions. In particular, coincidence of two resonances in [2, 3] was accompanied by full transmission in relatively wide frequency range around resonances, while resonance drops in S21 spectra disappeared. Meanwhile, approaching the 1st Kerker's condition should not be accompanied by such changes, since it should lead to a deep drop of BS and affect FS much less. Second question arises at the analysis of advertised in [3] phase shift by 2π in FS with respect to incident wave phase. Expectations of such shift were based on suggestion that in scattered waves two phase shifts by π in oscillations of electric and magnetic dipoles could be combined. However, this suggestion omits from consideration the fact that both shifts of the phase by π occur at two resonances with respect to the phase of incident wave and not with respect to the other resonance, thus keeping the resonances independent.

In this work, in order to address the above listed issues, additional investigations of arrays composed of silicon resonators have been conducted. In particular, transmission spectra of arrays have been simulated for both single cell models typically employed for MMs studies and for models used to analyze dispersion properties of photonic crystals (PhCs) and composed of stacked planar arrays. In addition, responses from arrays with various lattice constants at fixed diameters of disk resonators have been compared, while manipulating resonances in disks has been provided by changing their thicknesses. Dispersion diagrams of arrays were calculated by using the MPB software. Other simulations were performed by using COMSOL and CST Microwave Studio software packages.

II. Spectral Changes of MR, ER, and S21 at Varying Thickness of Silicon Disks in Arrays

Fig. 1 presents fragments of arrays under study with smallest and largest lattice parameters. While in first case distances between resonators were almost three times less than disk diameters, in second case they essentially exceeded these diameters. A plane wave was incident along z-axis, with E-field directed along x-axis and H-field-along y-axis.

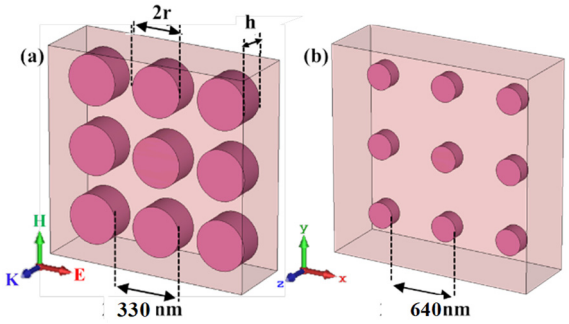

Fig. 1. 3 x 3 fragments of silicon disk arrays with lattice constants of (a) 330 nm (as in [3]) and (b) 640 nm. Disk radius is 120 nm and refractive index of silicon is 3.5. The disk thickness, *h*, could be varied from 40nm to 240nm.

This work was supported by the National Science Foundation under Award ECCS-1709991.

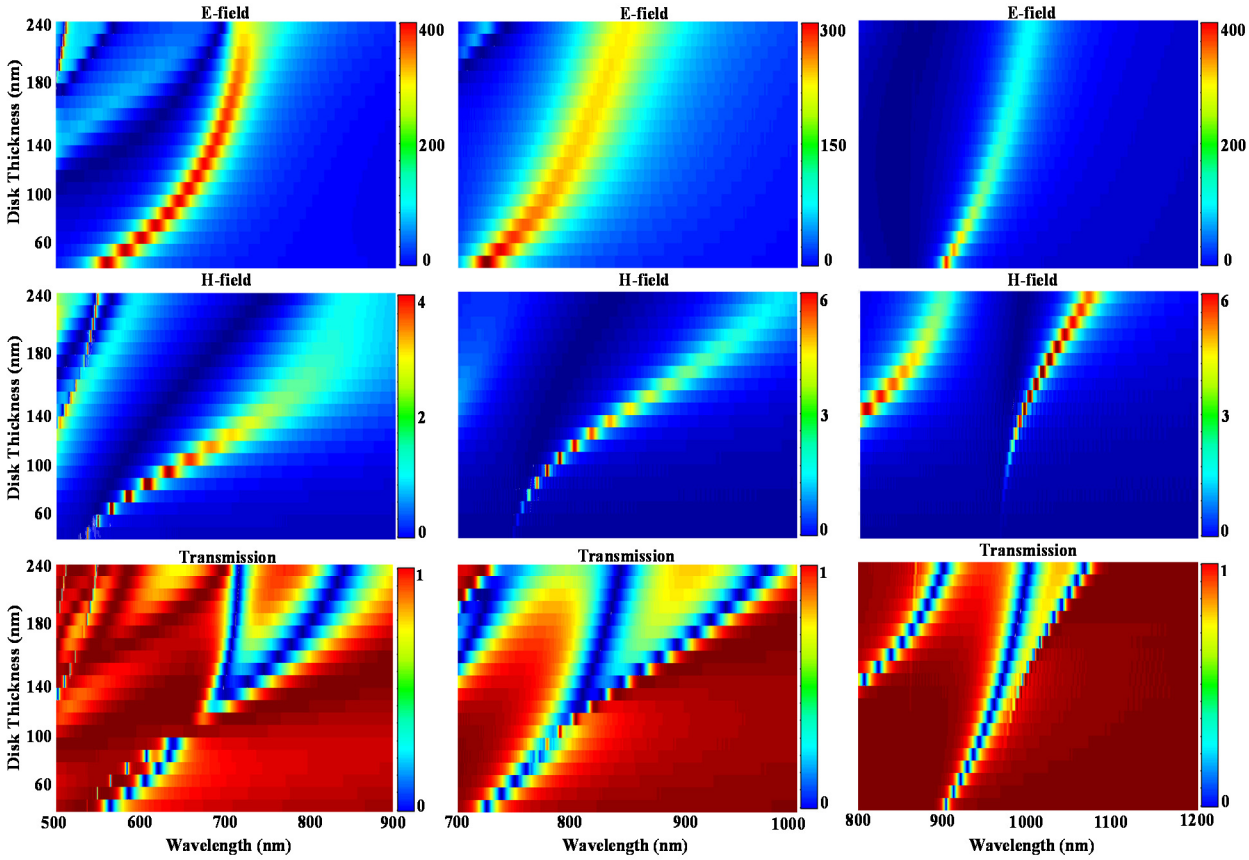

Fig. 2. Dependencies on disk thicknesses for spectral positions of ER (upper row), MR (2nd row), and color scaled S21 spectra (lower row) at array lattice constants α in nm: 1st column -330, 2nd column -480, and 3rd column -640. Disk radius is 120 nm.

Fig. 2 presents spectral positions of ERs and MRs, as well as color-scaled S21 spectra simulated for single unit cell models of silicon disk arrays in dependence on disk thickness *h*. The data in columns characterize arrays with different lattice constant α. As seen in Fig. 2, for all lattice constants, both resonances get stronger and more narrowband at decreasing the thickness of disks, however, in case of MR, this bandwidth decrease leads to resonance disappearance at small *h*. Transmission spectra in Fig. 2 show that spectral positions of ER and MR come closer at decreasing the thickness of disks, demonstrating a trend to coincide at *h* of 100-130 nm. At α =310 nm, coincidence of resonances looks accompanied by full transmission (S21 approaches 1), while at lower thicknesses of disks, the drops in S21 spectra, characteristic for resonance responses, become restored. In this range of disk thicknesses, the order, in which ER and MR appear in the spectra, is reversed, that point out at crossing of resonance curves of ER and MR at *h* of about 110 nm. These results seem confirming effects related to coincidence of ER and MR in [2, 3] despite of the serious doubts about compatibility of field distributions characterizing two dipolar resonances in dielectric particles. In addition, the data presented in Fig. 2 for arrays with bigger lattice constants reveal complications. It can be seen in 2nd column of pictures that at α =480 nm, S21 spectra do not demonstrate wide band of full transmission, and that there is no crossing of curves representing spectral positions of ER and MR. In favor of coincidence of two resonances only narrow spots with enhanced transmission within ER-related channel could be considered. Further, at α =640 nm (3rd column in Fig. 2), no effects related to coincidence of two resonances could be detected. Since tested increase of lattice constant had to make resonance processes in disks less dependent on interaction with neighbors, while this appeared to deteriorate resonance overlapping, it could be concluded that coincidence of resonances could not be achieved without strong integration of resonant processes in arrays. Such integration could be provided by coupling between resonances in neighboring disks [4], as well as by formation of Bloch's modes owing array periodicity. It is worth noting that all markers of ER and MR in Fig. 2 demonstrate meaningful shifts to lower frequencies at increase of lattice constants that apparently is a result of spreading resonance fields in sparse arrays compared to squeezed and distorted resonance fields

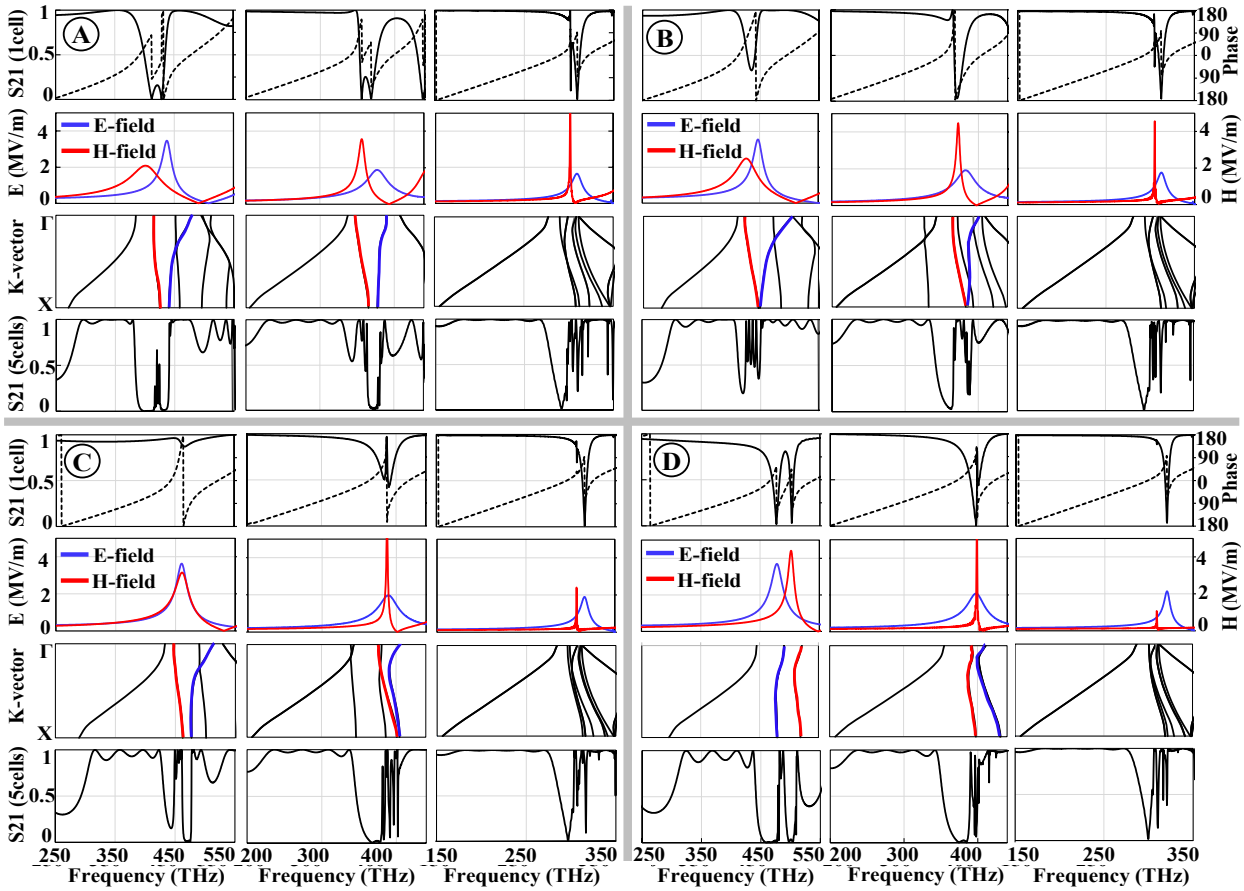

Fig. 3. Four groups A-D present the results for four types of arrays, which differ by the disk thickness, in nm: A-140, B-120, C-100, and D-80. Columns in each group represent arrays with different lattice constants, in nm: 1st column – 310, 2nd -480, 3rd -640. Four rows in each group(from top to bottom) present, respectively, S21 spectra for one cell model, E- and H- field probe signal spectra, dispersion diagrams, and S21 spectra for five arrays stacked in the direction of wave propagation.

in heavily packed arrays, which are incapable of confining longer wavelengths. It follows from the obtained results that observed MRs and ERs are not entirely defined by the disk geometry and material, instead they rater represent integrated array responses. Direct appeal to Kerker's conditions in this case could not be justified.

III. Responses of Single Planar Arrays Versus Responses of Stacked Arrays

Fig. 3 presents the data for arrays in four groups (A-D), which differ by the thickness *h* of disks. Three columns in each group represent subgroups, which differ by array lattice constant *a*. Rows of data in each group illustrate various types of array responses, in particular, S21 spectra for single cell model (upper rows) and S21 spectra for five planar arrays stacked in the direction of wave propagation (lower rows), probe signal spectra for E- and H-fields at single cell simulations (2nd rows) and the dispersion diagrams (3rd rows) calculated for infinite arrays.

As seen in the figure, S21 spectra for single cell models of planar arrays and for stacks of five arrays are essentially different for all cases under study. The single cell model is known to represent properties of arrays properly when all cells in arras and entire arrays respond identically that is assumed to take place in MMs. Observed discrepancy between the data for single cell models and for a stacks of arrays is characteristic, rather, for PhCs with typical for them dominance of dispersion phenomena [5]. For PhCs, dispersion diagrams calculated for infinite arrays, as expected, correspond well to simulated S21 spectra for stacks of five arrays. In particular, deep drops in S21 spectra are observed in all cases at the locations of bandgaps in dispersion diagrams, while locations of transmission branches in the latter correlate with observations of transmission bands in S21 spectra. Such correlation allows for suggesting that single planar arrays should also have some features represented by dispersion diagrams in Fig. 3. S21 spectra shown in 1st rows and probe signal spectra in 2nd rows of four groups in Fig. 3 are in favor of this

assumption. As seen in figure, the peaks in probe signal spectra representing two resonances in first two columns of all four groups in most cases can be associated with two specific transmission branches in dispersion diagrams, which are marked for clarity by the same colors as magnetic and electric resonance responses in probe signal spectra. At lower α values, those branches, which look associated with magnetic resonances, appear to demonstrate slopes characteristic for wave propagation with positive refractive indices. Just opposite, the branches, which look associated with electric resonances, demonstrate slopes typical for media with negative refraction indices. Based on these data, it could be suggested that colored branches in dispersion diagrams support resonance propagating modes [5], i.e represent integrated responses of arrays with strongly coupled resonators. Another observation that can be made regarding probe signal spectra presented in 2nd rows of four groups in Fig. 3 is that spectral responses at ERs and MRs have features characteristic for Fano-type resonances, in particular, they are asymmetric and drop down to zero above the resonances. The latter feature is typically related to destructive interference of waves produced by two sources. In the considered case, this process could involve waves scattered by two resonances, and, in such case, it should be affected by switching of phases of dipole oscillations by 180^0 at the resonance frequencies.

It can also be noticed in Fig. 3 that Q-factors of resonances, especially of MRs, increase essentially at the increase of lattice constant a that can be explained by the decrease of resonance field distortions in loosely packed arrays compared to such distortions in heavily packed arrays. To illustrate the difference in distortions, as well as in integration of resonance responses in arrays, Fig. 4 compares the distributions of E- and H- fields in 3 x 3 fragments of arrays with lattice constants of 330 nm and 640 nm at frequencies of MRs and ERs. This comparison is conducted for disks with the thickness of 140 nm. As seen in Fig. 4, electric dipoles in arrays with α=330 nm are strongly confined within the resonator bodies, while regions of E-fields providing coupling between neighbors in x-direction look squeezed in width down to 1/3 of disk diameter. Oppositely directed E-fields in the gaps between resonators in y-direction look, just opposite, largely enhanced. In arrays with α=640 nm, both confinement of electric dipoles and squeezing of field lines in inter-resonator gaps in y-directions appear decreased, while E-fields contributing to coupling along x-directions are enhanced. Magnetic dipoles in arrays with both small and large α seem less coupled then electric dipoles, however their fields continue to form laminar patterns confirming integration of responses from individual resonators.

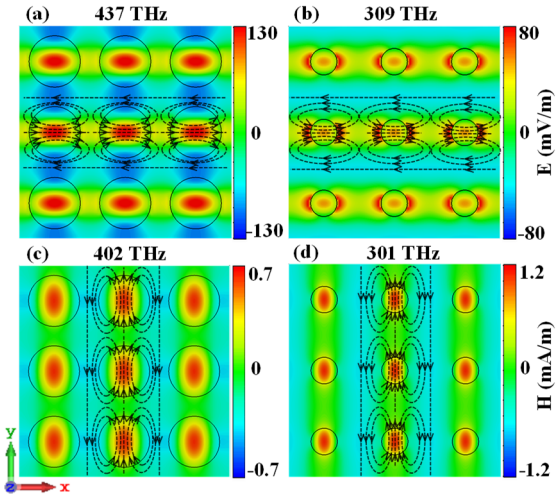

Fig. 4. (a, b) E-field and (c, d) H-field patterns in xy-cross-sections of 3x3 fragments of arrays with lattice constants of 330 nm (left column), and 640 nm (right column) at ERs and MRs observed, respectively, at (a) 437 THz, (b) 309 THz, and (c) 402 THz, (d) 301 THz. Disk radius – 120 nm, disk thickness – 140 nm.

IV. Conclusion

Obtained results contradict the consideration of metasurfaces of dielectric resonators as assembly of independent particles. Instead, it is shown that resonators in arrays are integrated by coupled fields. In addition, these arrays appear to have a lot in common with PhCs, in which array responses strongly depend on lattice parameters. Coincidence of MRs and ERs appears only in heavily packed arrays, so that transmission through arrays cannot be described by wave scattering from single particles. Investigated planar arrays cannot also be considered as MMs, i.e. homogenized media characterized by effective parameters. Analysis of array responses should account for their periodicity and dispersion properties.

References

[1] B. S. Luk`yanchuk, et al.,"Optimum forward light scattering by spherical and spheroidal dielectric nanoparticles with high refractive index", ACS Photonics, 2, 993–995, 2015.

[2] L. Staude, et al.,"Tailoring directional scattering through magnetic and electric resonances in subwavelength silicon nanodisks", ACS Nano, Vol.7, No.9, 7824–7832, 2013.

[3] Y. F. Yu et al., "High transmission dielectric meta-surfaces with 2π phase control at visible wavelengths", Laser Photonics Rev., 9, No.4, 412-418, 2015.

[4] F. Chen, X .Wang, G. Semouchkin, and E. Semouchkina, "Effects of Inductive Waves on Multi-Band below-cut-off Transmission in Waveguides Loaded with Dielectric Metamaterials,"*AIPAdvances*, 4, no. 10, p. 107129, 2014.

[5] N. P. Gandji, G. Semouchkin, and E. Semouchkina,"All-dielectric metamaterials: irrelevance of negative refraction to overlapping Mie resonances", J. Phys. D: Appl. Phys., 50, 455104, 2017.